Earth Systems and Environment (2019) 3:651–659
https://doi.org/10.1007/s41748-019-00109-w

ORIGINAL ARTICLE

Synthesis of Graphene Oxide/Silica/Carbon Nanotubes Composite for Removal of Dyes from Wastewater

Noha Almoisheer[1] · Fathia A. Alseroury[1,2] · Rajeev Kumar[3] · Talal Almeelbi[3] · M. A. Barakat[3,4]

Received: 20 March 2019 / Accepted: 3 August 2019 / Published online: 13 August 2019

Abstract

The recent interest in adsorption of pollutants on nanomaterials has been gaining widespread attention especially in the utilization of nanocarbon based composite materials. Herein, graphene oxide/silica/single-wall carbon nanotubes (GO/SiO_2/SWCNTs) composite was successfully prepared by a hydrothermal method for the adsorption of Congo red (CR) dye from synthetic wastewater. The nanocomposite morphology was characterized by X-ray diffraction (XRD), Field emission scanning electron microscope (FESEM), and Energy-dispersive X-ray spectroscopy (EDX). The present study focuses on the adsorption performance of CR dye from aqueous solution on GO/SiO_2/SWCNTs composite in terms of kinetics, isotherm, thermodynamics studies and optimization of factors such as pH, temperature, concentration and adsorption time. The results showed that a higher adsorption of CR was observed onto GO/SiO_2/SWCNT composite at pH 3.0 as compared to that with SiO_2 and SWCNT. Similarly, the maximum adsorption capacity of 456.15 mg g^{-1} was achieved at optimum temperature 20 °C, time (330 min) and 300 mg L^{-1} CR solution concentration. The dye adsorption on the nanocomposite was found to be obeying pseudo-second-order rate equation. Thermodynamic parameters showed that the adsorption of CR dye was spontaneous in nature.

Keywords GO/SiO_2/SWCNTs · Nanocomposite · Adsorption · Congo red dye · Kinetics · Isotherms · Wastewater

1 Introduction

Generally, dyes are present in the wastewater of multiple industries (Yao et al. 2010) such as textile, paint and plastics (Wang et al. 2012; Tan et al. 2015; Ahmad et al. 2015). The discharge of these dyes into water has a negative impact to the environment (de Carvalho et al. 2011) due to toxins even at low concentrations coupled with producing color of the receiving water (Mittal et al. 2009). One of the manufactured dyes existing in the water environment is Congo Red (CR) (Gharbani et al. 2008). CR is a benzidine derivative of azo dye (Pandey et al. 2018) which causes carcinogenic effects (Miandad et al. 2018) into aquatic living organisms and humans (Wanyonyi et al. 2014). Additionally, CR shows symptoms on both Digestive and Respiratory systems (Miandad et al. 2018). This dye has been removed from aquatic systems, to avoid their side effects, by several methods such as membrane separation, ozonization, photocatalysis and electrochemical method and adsorption (Molinari et al. 2004; Gharbani et al. 2008; Jain and Sikarwar 2006; Lachheb et al. 2002; Shaban et al. 2018). Adsorption procedure has been found to be highly effective and simple to operate than other methods (Shaban et al. 2018).

Different adsorbents have been used to treat wastewaters containing CR like activated carbons, clay, biomass, polymers, and zeolites (Namasivayam and Kavitha 2002; Vimonses et al. 2009; Han et al. 2008; Ozmen and Yilmaz 2007) and (Liu et al. 2014). Even so, their disadvantages, including separation inconvenience and low adsorption capacities, led to the need to investigate new promising adsorbents (Dehghani et al. 2013).

✉ M. A. Barakat
mabarakat@gmail.com

[1] Department of Physics, Faculty of Science, King Abdulaziz University, Jeddah, Kingdom of Saudi Arabia

[2] Department of Physics, Faculty of Science, University of Jeddah, Jeddah, Kingdom of Saudi Arabia

[3] Department of Environmental Sciences, Faculty of Meteorology, Environment and Arid Land Agriculture, King Abdulaziz University, Jeddah 21589, Kingdom of Saudi Arabia

[4] Central Metallurgical R&D Institute, Helwan 11421, Cairo, Egypt

In the same matter, carbon nanotubes (CNTs) have been investigated in water treatment (Gupta et al. 2013) due to its chemical and physical properties. CNTs has been proved in various studies for its ability to remove dyes in aqueous solution (Hamidi Malayeri et al. 2012). However, the application of CNTs may be limited (Sadegh et al. 2014) due to its expensive cost (Ong et al. 2010; Lu et al. 2016) and CNTs hydrophobic surface (Zare et al. 2015).

Graphene oxide (GO) as material showed potential adsorption toward water pollutants, in recent studies (Fan et al. 2012; Cheng et al. 2015). This behavior occurs due to the unique mechanical strength and large surface area of GO (Fan et al. 2012). However, the difficulty in separation after adsorption may limit the application of this material (Cheng et al. 2015).

One of the most porous membrane materials is Silica (SiO_2) (Jawaid and Khan 2018). Owing to its high surface area, SiO_2 material is not only considered perfect for surface modification but also has the ability to be a good adsorbent (Wang et al. 2018). Nanocomposites of silica incorporated with carbon nanotubes are effective in water treatment to remove heavy metals (Saleh 2015, 2016).

To overcome the above-mentioned disadvantages of Carbon nanotubes, some materials have been used to modify those tubes such as chitosan, graphene, and polymers (Chatterjee et al. 2010; Yu et al. 2014; Deng et al. 2013a; Gao et al. 2013). Nanocomposite has been successfully used in water treatment as removal/degradation of toxic dye (Jawaid and Khan 2018).

In this work, the target is to evaluate the adsorption performance of CR dye from aqueous solution on the synthesized GO/SiO_2/SWCNTs composite. Different parameters affecting the adsorption process were investigated such as pH, CR dye concentration, time and temperature.

2 Materials and Methods

Congo red (CR) dye was used as the model complex pollutant in the present study (Gharbani et al. 2008). CR general characteristics are molecular formula $C_{32}H_{22}N_6Na_2O_6S_2$, molecular mass as 696.68 g mol^{-1} (Panda et al. 2009) and maximum light adsorption $\lambda_{max} = 496$ nm (Deng et al. 2013b). This anionic dye was acquired from KOCK-LIGHT LABORATORIES LTD, Colnbrook-Bucks-England.

2.1 Adsorbent Synthesis

Single-walled carbon nanotubes (SWCNTs) (purity, 95%; average diameter, 1.1 nm; surface area, 450 m^2/g; and rang length 5–30 µm) were purchased from Beijing Deke Daojin Science and Technology Co., Ltd, China. The manufacturing method was the chemical vapor deposition (CVD). Tetraethyl othosilicate (TEOS) has been used to provide the silica particles (SiO_2) in the synthesis of GO/SiO_2/SWCNTs nanocomposite. (SiO_2) were obtained by the hydrolysis of 1.66 mL of (TEOS) in 25 mL of ethanol medium. Then, Graphene oxide (GO) was synthesized by Hummers' method. 15 mg of GO was added to 20 mL of water and sonicated for 2 h. After that, an amount of 1.1 g of single-walled carbon nanotubes (SWCNTs) was added to a solution of 1.2 g of Sodium dodecyl sulfate (SDS) in 20 mL of water. The mixture was stirred for 2 h. Thereafter, all the reagents were mixed and stirred for 3 h and further sonicated for 1 h. Then 12 mL ammonium solution was added dropwise under the continuous stirring condition for 2 h and transferred to the hydrothermal reactor and heated at 125 °C for 18 h. A black precipitated centrifuged and washed thoroughly with water, acetone and dried at 105 °C.

2.2 Characterization

Various technologies were applied for characterization of the synthesized materials (SWCNT, SiO_2 and the GO/SiO_2/SWCNTs). The materials were characterized by X-ray diffractometer (XRD; type Ultima-IV; Rigaku, Japan) with Cu Kα radiation (40 kV, 40 mA), with a wavelength of 0.154056 nm, over the range (2θ) from 10° to 80°. The surface morphology of the samples was elucidated by Field emission scanning electron microscope (FESEM) (JSM—7600F; JEOL—Japan) measurements operated at 5.0 kV. Energy-dispersive X-ray spectroscopy (EDX) was used for semi-quantitative elemental analysis of GO/SiO_2/SWCNTs composite.

2.3 Adsorption Experiments

The synthesized materials efficiency was studied for the removal of CR dye in a batch mode, by adding a fixed amount of absorbent (10 mg) into 20 mL of CR solution at a fixed concentration and the content pH ranging from 2 to 10 using 0.1 M HCl or/and 0.1 M NaOH. Thermodynamic and adsorption isotherm experiments were investigated by employing a series of CR concentration varied from 50 to 500 mg/L at three different temperatures (20 °C, 30 °C, and 40 °C). The adsorption equilibrium time studies were conducted at reaction times scaled in the range of 0–360 min and both pH and concentration were maintained constants. The initial and residual dye molecules concentration in CR solutions were analyzed by UV Spectrophotometer (UV-1800, Shimadzu, Japan) at 496 nm. The amount of CR adsorption per unit mass was determined based on the results of experiment, by the formula (Zazouli et al. 2013):

$$q_e = \frac{(C_0 - C_e)V}{m}, \quad (1)$$

where C_0 (mg/L)and C_e (mg/L)are the initial congo red dye concentration and the IC dye concentration in t time, respectively. q_e represent adsorption capacity (mg/g adsorbent). V and m are the sample volume in (L) and adsorbent mass in (g).

3 Results and Discussion

3.1 Characterization of Nanocomposite

The crystallinity and structure of the synthesized materials SWCNTs, SiO_2 and their nanocomposite GO/SiO_2/SWCNTs were subjected to XRD. The diffraction pattern for each material is represented in Fig. 1. The diffraction patterns are showing a good matching with the SWCNTs (Card No.-00-055-0161) and SiO_2 (Card No.-01-073-3466). It can be seen that these characteristic peaks for SWCNTs and SiO_2 existed in the XRD pattern of GO/SiO_2/SWCNTs nanocomposite.

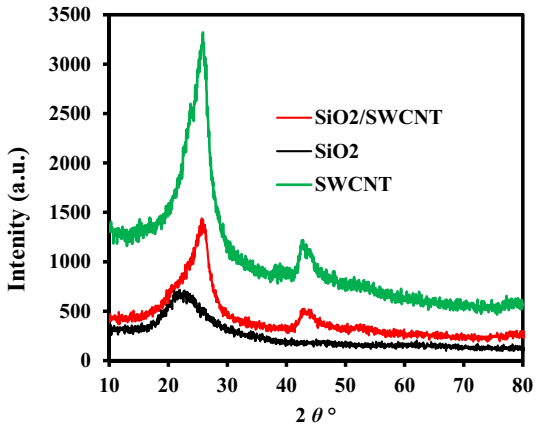

Fig. 1 XRD pattern of: **a** SWCNTs, **b** SiO_2 **c** GO/SiO_2/SWCNTs

The prepared nanocomposite showed a couple of diffraction crystalline peaks corresponding to (2θ) at 25.4° and 43.2°, which were also observed by Barakat et al. 2016.

The morphology and microstructure of the samples were observed using field emission scanning electron microscopy (FESEM), for SWCNTs, SiO_2 and their composite GO/SiO_2/SWCNTs adsorbents in Fig. 2. SEM image of pure SWCNTs clarifies the bundle like structure for SWCNTs (Fig. 2a), whereas pure SiO_2 showed the sphere-like morphology (Fig. 2b). A quit similar appearance of SiO_2 has also been observed by Hu et al. (2018). In the case of nanocomposite material, the SEM showed an entangled network of strips like morphology for SWCNTs interlinked with GO/SiO_2 (Fig. 2c).

To confirm the presence of the GO and SiO_2 in the composite, the EDX analysis of the GO/SiO_2/SWCNTs composite is compared as shown in Table 1. The EDX measurements revealed both carbon (95%) and oxygen (5%) in the elemental composition of pure SWCNTs, and both silicon (66.67%) and oxygen (33.33%) in the elemental composition of pure SiO_2. After the modification of SWCNTs with GO/SiO_2, the elemental composition of the GO/SiO_2/SWCNTs composite is C (63.42%), O (24.59%) and Si (11.99%), respectively.

Table 1 Elemental composition of pure SWCNTs (Kuhn et al. 2013), pure GO (Chen et al. 2012), pure SiO_2 (Rohaeti 2015) and GO/SiO_2/SWCNTs

Element	Pure SWCNT wt%	Pure GO wt%	Pure SiO_2 wt%	GO/SiO_2/SWCNTs wt%
C	95	67.75	–	63.42
O	5	32.25	66.67	24.59
Si	–	–	33.33	11.99

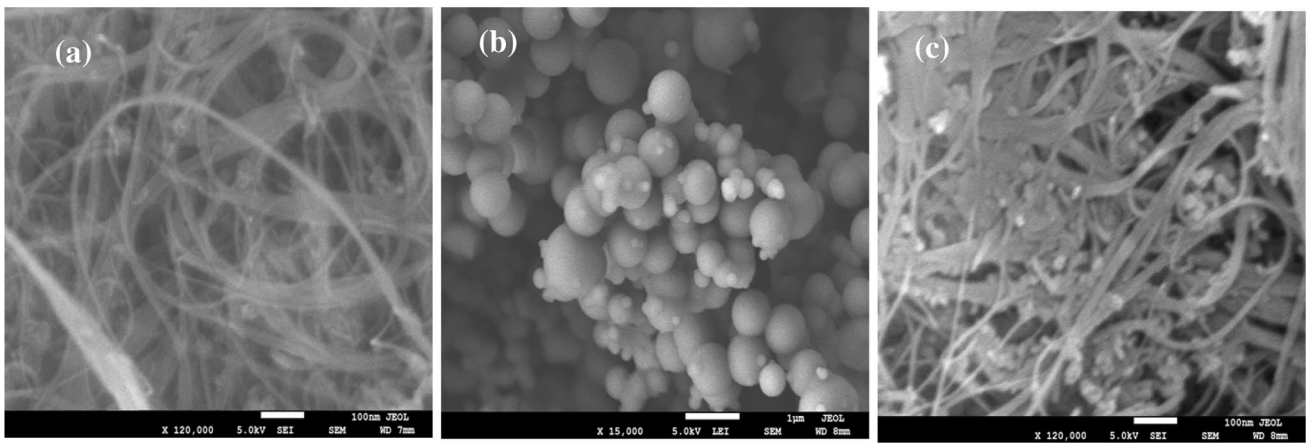

Fig. 2 SEM images of: **a** SWCNTs, **b** SiO_2 **c** GO/SiO_2/SWCNTs

3.2 Adsorption Study

3.2.1 Effect of pH

The effect of solution pH of CR dye removal using GO/SiO_2/SWCNT composite was studied and compared with the SWCNT and SiO_2 materials. The experiment was performed at 20 °C using 0.01 g of the adsorbent material in 20 mL CR solution (200 mg/L CR concentration). The testing pH range was between 3 and 10 (Fig. 3), Results obtained indicate that the maximum value of CR adsorption capacity was attained by GO/SiO_2/SWCNT. The maximum CR adsorption of 456.15 mg/g was achieved within 330 min of constant time under the optimum pH 3.0, temperature 20 °C and CR concentration of 300 mg/L. On another hand, utilizing SiO_2 and SWCNT gave a lower adsorption capacity was found at all pH ranges.

This phenomenon can be explained on the basis of the surface property of the GO/SiO_2/SWCNT composite and different ionic forms of the CR in aqueous solution (Barakat et al. 2016). At low pH, the surface of the nanocomposite (GO/SiO_2/SWCNTs) become more positive by an increase in the H^+ ion concentration (Miandad et al. 2018). An electrostatic interaction between the protonated surface of nanocomposite (GO/SiO_2/SWCNTs) and CR dye causes a maximum adsorption of Congo red dye at pH 3 (Zulfikar and Setiyanto 2013; Miandad et al. 2018). With the solution having higher pH, the surface of nanocomposite (GO/SiO_2/SWCNTs) become negative due to the decreasing of H^+ ion and more positive ions leave the OH from the nanocomposite surface (Miandad et al. 2018). Therefore, there was a decrease of CR removal by a strong electrostatic repulsion between CR and adsorbent surface (Miandad et al. 2018). At the same time, a measurable amount of CR adsorption occurred could be explained by considering other adsorption mechanisms, such as hydrogen bonds and π–π interaction with the C=C (Pavan et al. 2008).

3.2.2 Effects of Initial CR Concentration and Temperature

Figure 4 shows the removal of CR dye by GO/SiO_2/SWCNT composite at multiple temperatures (20 °C, 30 °C, and 40 °C) for different initial CR concentration from 50 to 500 mg L^{-1}. According to Mittal et al. 2009, if the adsorption of Congo Red by the nanocomposite is increased with the increase in the initial CR concentration of the solute, then the concentration of CR solution has a huge influence onto adsorption process. At 300 mg L^{-1}, the adsorption capacity of CR decreased from 422.26 to 241.2 mg g^{-1} onto GO/SiO_2/SWCNT composite with increasing solution temperature from 20 to 40 °C. The worsen performance could be attributed to the deformation of the adsorption sites on the adsorbent GO/SiO_2/SWCNT surface owing to the increase in temperature (Kumar et al. 2015).

3.3 Adsorption Isotherms

Adsorption isotherm analysis is depicting the relationship of amount adsorbed by a unit weight of adsorbent with the concentration of adsorbent remaining in the medium at equilibrium (Purkait et al. 2007; Mittal et al. 2009; Kumar et al. 2019). Langmuir (Kumar et al. 2015) and Freundlich (de Carvalho et al. 2011) isotherms consider common models for a better illustration of Congo Red adsorption process (Kumar et al. 2015). The applicability of Langmuir model is indicative where the monolayer coverage of CR dye on the surface of nanocomposite different from the applicability Freundlich model which is indicated where the heterogeneous surface of the nanocomposite (Purkait et al. 2007). Langmuir isotherm

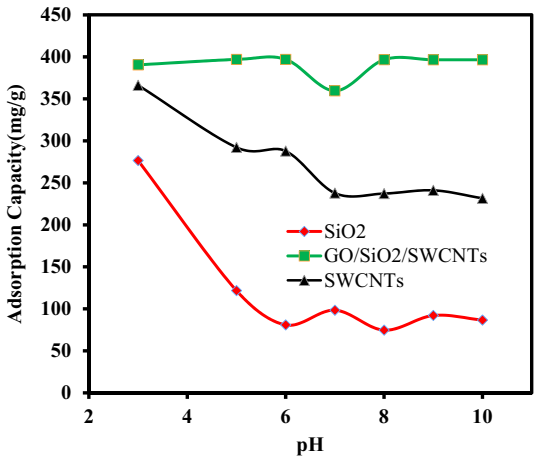

Fig. 3 Effect of pH on adsorption on to SWCNTs, SiO_2 and GO/SiO_2/SWCNTs (Conc.-200 mg L^{-1}, V-20 mL, Temp.-20 °C, Time 6 h, m-0.01 g)

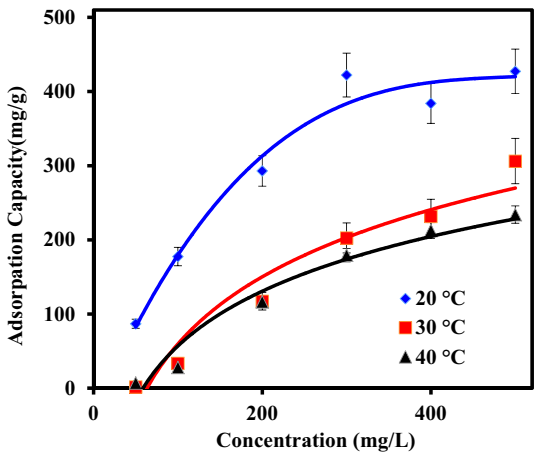

Fig. 4 Effect of initial CR concentration and temperature on adsorption (V-20 mL, Time-6 h, m-0.01 g, pH-3)

is expressed by Eq. (2) and Freundlich isotherm is expressed by Eq. (3) (de Carvalho et al. 2011)

$$\frac{1}{q_e} = \frac{1}{C_e K_L q_m} + \frac{1}{q_m}, \tag{2}$$

$$\ln q_e = \frac{1}{n} \ln C_e + K_F, \tag{3}$$

where q_m (mg/g) is the maximum monolayer adsorption capacity and K_L (L/mg) is the free energy of adsorption. Both q_m (mg/g) and K_L (L/mg) are the Langmuir constant. C_e (mg/L) is the CR concentration at equilibrium. At the same time, the Freundlich constant are K_F adsorption capacity and n adsorption intensity. Figures 5 and 6 show the plot of the experimental data based on both isotherms models. At each temperature, Langmuir and Freundlich constants are presented in Table 2. The comparison between coefficient values (R^2) of both models reveled that CR adsorbed through monolayer coverage onto GO/SiO_2/SWCNT with maximum capacity value (q_m) of 555.55 mg/g at 20 °C. In our experimental range, the results of nanocomposite are best described using the Langmuir model.

3.4 Adsorption Thermodynamics

To get further information regarding the inherent energetic changes into the adsorption mechanism, the change in standard free energy ($\Delta G°$), entropy ($\Delta S°$), and enthalpy ($\Delta H°$) have been calculated from Van't Hoff and Gibbs equations expressed by Eqs. (4) and (5), respectively (Ho and Ofomaja 2006):

$$\ln K_L = \frac{\Delta S°}{R} - \frac{\Delta H°}{RT}, \tag{4}$$

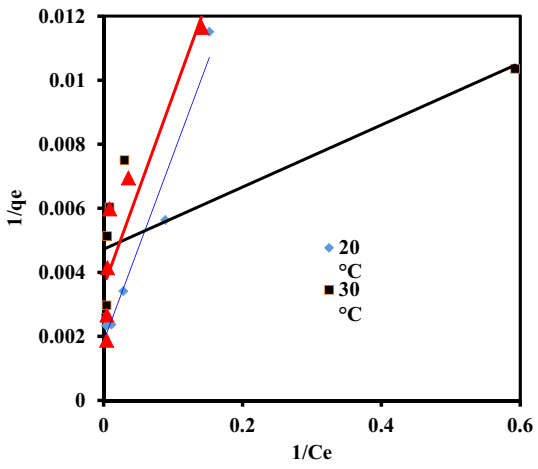

Fig. 5 Langmuir isotherm plot for adsorption of congo red by GO/SiO_2/SWCNTs

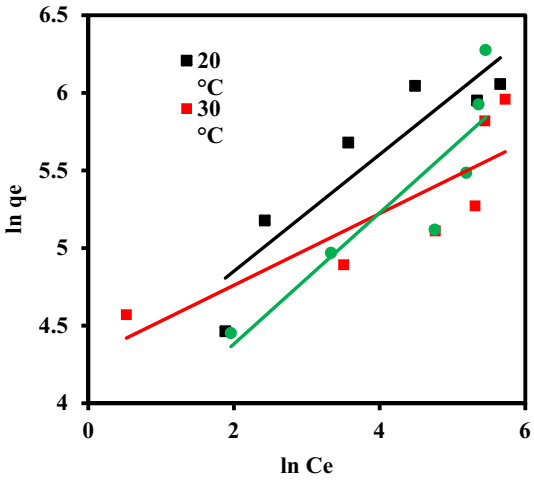

Fig. 6 Freundlich isotherm plot for adsorption of congo red by GO/SiO_2/SWCNTs

$$\Delta G° = -RT \ln K_L, \tag{5}$$

where R is the universal gas constant, 8.314 J/mol K, T is temperature (K), and K_L is the Langmuir adsorption equilibrium constant.

A Van't Hoff plot was calculated, the parameters $\Delta S°$, $\Delta H°$ and $\Delta G°$ for the adsorption of CR on the prepared nanocomposite were shown in Table 3. In view of the intercept and slope of the Van't Hoff plot, the values of $\Delta S°$ and $\Delta H°$ were resolved. The former value indicates an increment in randomness at the solid/solution interface during the absorption of CR dye onto GO/SiO2/SWCNTs composite (Ho and Ofomaja 2006). Furthermore, the latter suggests the exothermic (Ojedokun and Bello 2017). In addition, $\Delta G°$ was calculated using K_L Langmuir constant expressed in (mol/g). This value suggests the spontaneous nature of the adsorption on nanocomposite (Ojedokun and Bello 2017).

3.5 Effect of Time

To determine the required time at which adsorption have the maximum value, the effect of time on the adsorption of CR on GO/SiO_2/SWCNT composite was studied as illustrated in Fig. 7a. The plot shows that the uptake of CR increases with time due to active sites significantly available. At 330 min, it reached a constant value, of 456.15 mg/g, beyond which the adsorption reached saturation state. In other words, the amount of dye molecules adsorbed at the equilibrium time reflected the maximum adsorption of CR on the GO/SiO_2/SWCNT composite (Tan et al. 2009; Miandad et al. 2018).

Table 2 Adsorption isotherm parameters for the removal of CR onto GO/SiO_2/SWCNT

Temp. °C	Langmuir isotherm model			Freundlich isotherm model		
	Q_m (mg g^{-1})	K_L (L mg^{-1})	R^2	K_F ($mg^{1-1/n}$ $L^{1/n}g^{-1}$)	N	R^2
20	555.55	0.0309	0.9554	60.364	2.661	0.8385
30	212.765	0.4845	0.6278	73.640	4.334	0.7204
40	277.77	0.0602	0.8330	34.484	2.371	0.7939

Table 3 Thermodynamics parameters for CR adsorption onto GO/SiO_2/SWCNTs composite

Temperature (°C)	$\Delta G°$ kJ mol^{-1}	$\Delta S°$ J $mol^{-1}K^{-1}$	$\Delta H°$ kJ mol^{-1}
20	−24.31821	0.19341	30.6337
30	−32.08334		
40	−27.711959		

3.6 Adsorption Kinetics

To examine the rate of CR dye adsorption onto GO/SiO_2/SWCNT composite, pseudo-first order and pseudo-second-order kinetic models were applied (Enaime et al. 2017; Kumar et al. 2015) given by Eqs. (6) and (7);

$$\log\left(q_e - q_t\right) = \log q_e - \frac{k_1 t}{2.303}, \tag{6}$$

$$\frac{t}{q_t} = \frac{1}{k_2 q_e^2} + \frac{t}{q_e}, \tag{7}$$

where q_t (mg g^{-1}) is the adsorption capacity at time t (min), q_e (mg g^{-1}) is the adsorption capacity at equilibrium, k_1 is the pseudo-first order rate constant (min^{-1}) and k_2 (g $mg^{-1}min^{-1}$) is the pseudo-second order rate constant. Linear fit plots of both models for the adsorption of CR dye are shown in Fig. 7b, c. The kinetic parameters and correlation coefficients for both equations are shown in Table 4. Comparing models reveals that the experimental kinetic data fit well with the pseudo-second order kinetic model, not only because of its high correlation coefficient value but also the fact that the $q_e^{(cal)}$ value is the closest to $q_e^{(exp)}$ value. (Kumar et al. 2015).

3.7 Comparison of Adsorption Capacities

The removal efficiency of the CR onto GO/SiO_2/SWCNTs composite has been compared with various kinds of adsorbents as reported in the literature. The results presented in Table 5 reveled that GO/SiO_2/SWCNTs composite is an efficient material for the removal of the CR as compared to the other adsorbents.

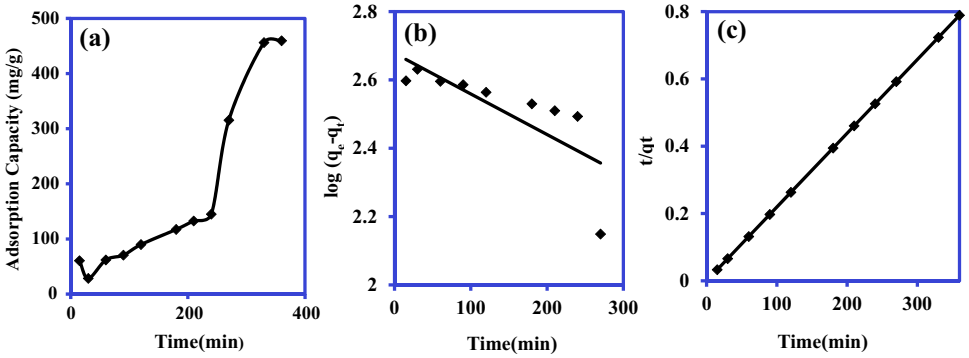

Fig. 7 Effect of time on CR dye adsorption onto GO/SiO_2/SWCNTs composite (m-0.01 g, V-20 mL, Temp.-20 °C, Conc.300 $mg.L^{-1}$) **a** Adsorption time effect, **b** Pseudo-first order, **c** Pseudo-second order adsorption kinetics of CR onto GO/SiO2/SWCNTs

Table 4 Kinetic parameters for CR adsorption onto GO/SiO_2/SWCNTs composite

$Q_e^{(exp)}$ (mg g^{-1})	Pseudo-first order model			Pseudo-second order model		
	$Q_e^{(cal)}$ (mg g^{-1})	K_1 (min^{-1})	R^2	$Q_e^{(cal)}$ (mg g^{-1})	K_2 (g $mg^{-1}min^{-1}$)	R^2
456.1553	476.32	0.0027636	0.58747	454.5454	0.0024	1

Table 5 The maximum monolayer adsorption capacity of various adsorbent used for adsorption of CR dye

Adsorbent	Adsorption capacity (mg/g)	pH	Conc. (mg/L)	References
Fe_2O_3	253.8	–	100	(Hao et al. 2014)
MIL-68 (In) nanorods	1204	2–10	50	(Jin et al. 2015)
Chitosan/montmorillonite	53.42	7.0	–	(Ngah et al. 2011)
γ-Fe_2O3	208.33	5.9	–	(Afkhami and Moosavi 2010)
CeO_2	942.7	–	100	(Ouyang et al. 2013)
MWCNTs	352.11	11	200	(Zare et al. 2015)
GO/SiO_2/SWCNTs	455.35	3	300	This work

4 Conclusion

This study reveals that the GO/SiO_2/SWCNTs composite was successively prepared as an efficient adsorbent for the removal of congo red dyes from aqueous solution. The XRD patterns, EDX analysis and SEM images proved the successful synthesis of GO/SiO_2/SWCNTs nanocomposite. The results showed that a higher adsorption capacity (390 mg g^{-1}) of CR was observed onto GO/SiO_2/SWCNT composite at pH 3.0 as compared to that with SiO_2 and SWCNT. The maximum CR adsorption of 456.15 mg g^{-1} was achieved within 330 min of constant time under the optimum pH 3.0, temperature 20 °C and CR concentration of 300 mg/L. The monolayer adsorption capacity of GO/SiO_2/SWCNTs nanocomposite for CR reduced from 555.55 to 277.77 mg/g as the solution temperature increases from 20 to 40 °C. The ongoing process proceeds via a pseudo-second-order mechanism for the absorbent with a high correlation coefficient. The thermodynamic parameters $\Delta G°$, $\Delta S°$ and $\Delta H°$ for the adsorption of congo red on nanocomposite are determined. The negative values of free energy $\Delta G°$ indicate the spontaneity, whereas the positive value of $\Delta S°$ signifies the increase in randomness of the process.

References

Afkhami A, Moosavi R (2010) Adsorptive removal of Congo red, a carcinogenic textile dye, from aqueous solutions by maghemite nanoparticles. J Hazard Mater 174(1–3):398–403

Ahmad A, Mohd-Setapar S, Chuong C, Khatoon A, Wani W, Kumar R, Rafatullah M (2015) Recent advances in new generation dye removal technologies: novel search for approaches to reprocess wastewater. RSC Adv 5(39):30801–30818

Barakat MA, Al-Ansari AM, Kumar R (2016) Synthesis and characterization of Fe–Al binary oxyhydroxides/MWCNTs nanocomposite for the removal of Cr(VI) from aqueous solution. J Taiwan Inst Chem Eng 63:303–311. https://doi.org/10.1016/j.jtice.2016.03.019

Chatterjee S, Lee MW, Woo SH (2010) Adsorption of congo red by chitosan hydrogel beads impregnated with carbon nanotubes. Biores Technol 101(6):1800–1806

Chen L, Chai S, Liu K, Ning N, Gao J, Liu Q, Fu Q (2012) Enhanced epoxy/silica composites mechanical properties by introducing graphene oxide to the interface. ACS Appl Mater Interfaces 4(8):4398–4404

Cheng Z, Liao J, He B, Zhang F, Zhang F, Huang X, Zhou L (2015) One-step fabrication of graphene oxide enhanced magnetic composite gel for highly efficient dye adsorption and catalysis. ACS Sustain Chem Eng 3(7):1677–1685

de Carvalho T, Fungaro D, Magdalena C, Cunico P (2011) Adsorption of indigo carmine from aqueous solution using coal fly ash and zeolite from fly ash. J Radioanal Nucl Chem 289(2):617–626

Dehghani MH, Naghizadeh A, Rashidi A, Derakhshani E (2013) Adsorption of reactive blue 29 dye from aqueous solution by multiwall carbon nanotubes. Desalin Water Treat 51(40–42):7655–7662

Deng C, Fu H, Teng L, Hu Z, Xu X, Chen J, Ren T (2013a) Antitumor activity of the regenerated triple-helical polysaccharide from Dictyophora indusiata. Int J Biol Macromol 61:453–458. https://doi.org/10.1016/j.ijbiomac.2013.08.007

Deng JH, Zhang XR, Zeng GM, Gong JL, Niu QY, Liang J (2013b) Simultaneous removal of Cd (II) and ionic dyes from aqueous solution using magnetic graphene oxide nanocomposite as an adsorbent. Chem Eng J 226:189–200. https://doi.org/10.1016/j.cej.2013.04.045

Enaime G, Ennaciri K, Ounas A, Baçaoui A, Seffen M, Selmi T, Yaacoubi A (2017) Preparation and characterization of activated carbons from olive wastes by physical and chemical activation: application to Indigo carmine adsorption. J Mater Environ Sci 8(11):4125–4137

Fan L, Luo C, Li X, Lu F, Qiu H, Sun M (2012) Fabrication of novel magnetic chitosan grafted with graphene oxide to enhance adsorption properties for methyl blue. J Hazard Mater 215:272–279

Gao H, Zhao S, Cheng X, Wang X, Zheng L (2013) Removal of anionic azo dyes from aqueous solution using magnetic polymer multi-wall carbon nanotube nanocomposite as adsorbent. Chem Eng J 223:84–90. https://doi.org/10.1016/j.cej.2013.03.004

Gharbani P, Tabatabaii SM, Mehrizad A (2008) Removal of Congo red from textile wastewater by ozonation. Int J Environ Sci Technol 5(4):495–500

Gupta VK, Kumar R, Nayak A, Saleh TA, Barakat MA (2013) Review article; adsorptive removal of dyes from aqueous solution onto carbon nanotubes: a review. Adv Coll Interface Sci 193:24–34. https://doi.org/10.1016/j.cis.2013.03.003

Hamidi Malayeri F, Sohrabi MR, Ghourchian H (2012) Magnetic multi-walled carbon nanotube as an adsorbent for toluidine blue o removal from aqueous solution. Int J Nanosci Nanotechnol 8(2):79–86

Han R, Ding D, Xu Y, Zou W, Wang Y, Li Y, Zou L (2008) Use of rice husk for the adsorption of congo red from aqueous solution in column mode. Bioresour Technol 99(8):2938–2946

Hao T, Yang C, Rao X, Wang J, Niu C, Su X (2014) Facile additive-free synthesis of iron oxide nanoparticles for efficient adsorptive removal of Congo red and Cr(VI). Appl Surf Sci 292:174–180. https://doi.org/10.1016/j.apsusc.2013.11.108

Ho YS, Ofomaja AE (2006) Biosorption thermodynamics of cadmium on coconut copra meal as biosorbent. Biochem Eng J 30(2):117–123

Hu M, Yan X, Hu X, Zhang J, Feng R, Zhou M (2018) Ultra-high adsorption capacity of MgO/SiO_2 composites with rough surfaces for Congo red removal from water. J Colloid Interface Sci 510:111–117. https://doi.org/10.1016/j.jcis.2017.09.063

Jain R, Sikarwar S (2006) Photocatalytic and adsorption studies on the removal of dye Congo red from wastewater. Int J Environ Pollut 27(1–3):158–178

Jawaid M, Khan MM (2018) Polymer-based nanocomposites for energy and environmental applications. Woodhead Publishing, Cambridge

Jin LN, Qian XY, Wang JG, Aslan H, Dong M (2015) MIL-68 (In) nano-rods for the removal of Congo red dye from aqueous solution. J Colloid Interface Sci 453:270–275. https://doi.org/10.1016/j.jcis.2015.05.005

Kuhn JN, Muralidharan R, Li X, Goswami DY, Stefanakos EK (2013) Reversible hydrogen storage in the LieMgeNeH system e The effects of Ru doped single walled carbon nanotubes on NH3 emission and kinetics. Int J Hydrogen Energy 38(10039):e10049

Kumar R, Ansari MO, Parveen N, Barakat MA, Cho MH (2015) Simple route for the generation of differently functionalized PVC@graphene–polyaniline fiber bundles for the removal of Congo red from wastewater. RSC Adv 5(76):61486–61494

Kumar R, Laskar MA, Hewaidy IF, Barakat MA (2019) Modified adsorbents for removal of heavy metals from aqueous environment: a review. Earth Syst Environ 3:83–93

Lachheb H, Puzenat E, Houas A, Ksibi M, Elaloui E, Guillard C, Herrmann JM (2002) Photocatalytic degradation of various types of dyes (Alizarin S, Crocein Orange G, Methyl Red, Congo Red, Methylene Blue) in water by UV-irradiated titania. Appl Catal B 39(1):75–90

Liu S, Ding Y, Li P, Diao K, Tan X, Lei F, Huang Z (2014) Adsorption of the anionic dye Congo red from aqueous solution onto natural zeolites modified with *N*,*N*-dimethyl dehydroabietylamine oxide. Chem Eng J 248:135–144. https://doi.org/10.1016/j.cej.2014.03.026

Lu H, Wang J, Stoller M, Wang T, Bao Y, Hao H (2016) Review article; An overview of nanomaterials for water and wastewater treatment. Adv Mater Sci Eng 2016:1–10. https://doi.org/10.1155/2016/4964828

Miandad R, Kumar R, Barakat MA, Basheer C, Aburiazaiza AS, Nizami AS, Rehan M (2018) Untapped conversion of plastic waste char into carbon-metal LDOs for the adsorption of Congo red. J Colloid Interface Sci 511:402–410. https://doi.org/10.1016/j.jcis.2017.10.029

Mittal A, Mittal J, Malviya A, Gupta VK (2009) Adsorptive removal of hazardous anionic dye "Congo red" from wastewater using waste materials and recovery by desorption. J Colloid Interface Sci 340(1):16–26

Molinari R, Pirillo F, Falco M, Loddo V, Palmisano L (2004) Photocatalytic degradation of dyes by using a membrane reactor. Chem Eng Process 43(9):1103–1114

Namasivayam C, Kavitha D (2002) Removal of Congo Red from water by adsorption onto activated carbon prepared from coir pith, an agricultural solid waste. Dyes Pigm 54(1):47–58

Ngah WW, Teong LC, Hanafiah MAKM (2011) Review article; Adsorption of dyes and heavy metal ions by chitosan composites: a review. Carbohyd Polym 83(4):1446–1456

Ojedokun AT, Bello OS (2017) Kinetic modeling of liquid-phase adsorption of Congo red dye using guava leaf-based activated carbon. Appl Water Sci 7(4):1965–1977

Ong YT, Ahmad AL, Zein SHS, Tan SH (2010) Review Article; A review on carbon nanotubes in an environmental protection and green engineering perspective. Braz J Chem Eng 27(2):227–242

Ouyang X, Li W, Xie S, Zhai T, Yu M, Gan J, Lu X (2013) Hierarchical CeO_2 nanospheres as highly-efficient adsorbents for dye removal. New J Chem 37(3):585–588

Ozmen EY, Yilmaz M (2007) Use of β-cyclodextrin and starch based polymers for sorption of Congo red from aqueous solutions. J Hazard Mater 148(1–2):303–310

Panda GC, Das SK, Guha AK (2009) Jute stick powder as a potential biomass for the removal of congo red and rhodamine B from their aqueous solution. J Hazard Mater 164(1):374–379

Pandey G, Singh S, Hitkari G (2018) Synthesis and characterization of polyvinyl pyrrolidone (PVP)-coated Fe_3O_4 nanoparticles by chemical co-precipitation method and removal of Congo red dye by adsorption process. Int Nano Lett 8:111–121. https://doi.org/10.1007/s40089-018-0234-6

Pavan FA, Dias SL, Lima EC, Benvenutti EV (2008) Removal of Congo red from aqueous solution by anilinepropylsilica xerogel. Dyes Pigments 76(1):64–69.

Purkait MK, Maiti A, Dasgupta S, De S (2007) Removal of congo red using activated carbon and its regeneration. J Hazard Mater 145(1–2):287–295

Rohaeti E (2015) Reduction of high purity silicon from bamboo leaf as basic material in development of sensors manufacture in satellite technology. Proc Environ Sci 24:308–316. https://doi.org/10.1016/j.proenv.2015.03.040

Sadegh H, Shahryari-ghoshekandi R, Kazemi M (2014) Study in synthesis and characterization of carbon nanotubes decorated by magnetic iron oxide nanoparticles. Int Nano Lett 4(4):129–135

Saleh TA (2015) Mercury sorption by silica/carbon nanotubes and silica/activated carbon: a comparison study. J Water Supply Res Technol Aqua 64(8):892–903

Saleh TA (2016) Nanocomposite of carbon nanotubes/silica nanoparticles and their use for adsorption of Pb(II): from surface properties to sorption mechanism. Desalin Water Treat 57(23):10730–10744

Shaban M, Sayed MI, Shahien MG, Abukhadra MR, Ahmed ZM (2018) Adsorption behavior of inorganic-and organic-modified kaolinite for Congo red dye from water, kinetic modeling, and equilibrium studies. J Sol-Gel Sci Technol 87:427–441. https://doi.org/10.1007/s10971-018-4719-6

Tan IAW, Ahmad AL, Hameed BH (2009) Adsorption isotherms, kinetics, thermodynamics and desorption studies of 2,4,6-trichlorophenol on oil palm empty fruit bunch-based activated carbon. J Hazard Mater 164(2–3):473–482

Tan KB, Vakili M, Horri BA, Poh PE, Abdullah AZ, Salamatinia B (2015) Adsorption of dyes by nanomaterials: recent developments and adsorption mechanisms. Sep Purif Technol 150:229–242. https://doi.org/10.1016/j.seppur.2015.07.009

Vimonses V, Lei S, Jin B, Chow CW, Saint C (2009) Kinetic study and equilibrium isotherm analysis of Congo Red adsorption by clay materials. Chem Eng J 148(2–3):354–364

Wang L, Li J, Wang Y, Zhao L, Jiang Q (2012) Adsorption capability for Congo red on nanocrystalline MFe2O4 (M = Mn, Fe Co, Ni) spinel ferrites. Chem Eng J 181:72–79. https://doi.org/10.1016/j.cej.2011.10.088

Wang J, Liu M, Chen T, Chen J, Ge W, Fu Z, Lu Y (2018) Core-shelled mesoporous $CoFe_2O_4$–SiO_2 material with good adsorption and

high-temperature magnetic recycling capabilities. J Phys Chem Solids 115:300–306. https://doi.org/10.1016/j.jpcs.2017.12.056

Wanyonyi WC, Onyari JM, Shiundu PM (2014) Adsorption of Congo Red Dye from aqueous solutions using roots of Eichhornia crassipes: kinetic and equilibrium studies. Energy Proc 50:862–869. http://hdl.handle.net/123456789/1049

Yao Y, Xu F, Chen M, Xu Z, Zhu Z (2010) Adsorption behavior of methylene blue on carbon nanotubes. Bioresour Technol 101(9):3040–3046

Yu JG, Zhao XH, Yang H, Chen XH, Yang Q, Yu LY, Chen XQ (2014) Review Article; Aqueous adsorption and removal of organic contaminants by carbon nanotubes. Sci Total Environ 482:241–251. https://doi.org/10.1016/j.scitotenv.2014.02.129

Zare K, Sadegh H, Shahryari-Ghoshekandi R, Maazinejad B, Ali V, Tyagi I, Gupta VK (2015) Enhanced removal of toxic Congo red dye using multi walled carbon nanotubes: kinetic, equilibrium studies and its comparison with other adsorbents. J Mol Liq 212:266–271. https://doi.org/10.1016/j.molliq.2015.09.027

Zazouli MA, Balarak D, Mahdavi Y, Ebrahimi M (2013) Adsorption rate of 198 reactive red dye from aqueous solutions by using activated red mud. Iran J Health Sci 1(1):36–43

Zulfikar MA, Setiyanto H (2013) Adsorption of congo red from aqueous solution using powdered eggshell. Int J Chem Tech Res 5(4):1532–1540